PHAGE: Therapy, Applications, and Research
Volume 6, Number 3, 2025

DOI: 10.1177/26416549251371574

Research Articles

The Role of Resuscitating Promoting Factors in Facilitating Infection of *Mycobacterium smegmatis* with Virulent Soil Bacteriophages

Chandni Madhav, MSc,[1,†] Khel Gordhan,[2,†] Nday Lucie Sungu, BSc (Hons),[1,†] Edith E. Machowski, PhD,[1] Christopher S. Ealand, PhD,[1] Bhavna Gowan Gordhan, PhD,[1] and Bavesh Davandra Kana, PhD[1]

Abstract

Background: Mycobacteriophages targeting *Mycobacterium tuberculosis*, show promise as adjuncts for treating drug resistant tuberculosis. While mycobacteriophages encode mycobacterial cell wall degrading enzymes, their interaction with the host during infection is poorly understood. In other bacteria, lytic transglycosylases, homologous to mycobacterial resuscitation-promoting factor, RpfB, have been implicated in facilitating infection. Given the multiplicity of Rpf homologues in mycobacteria, we explored their individual and combined roles in mycobacteriophage infection.
Materials and Methods: Soil-derived mycobacteriophages, MontyDev and Bora were isolated and tested on *Mycobacterium smegmatis* strains carrying various *rpf* gene deletions.
Results: Complete loss of Rpf proteins led to ~75% reduction in plaque formation, which was reversed by complementation with specific Rpf proteins. RfpC, RpfD, and RpfE were dispensable for bacteriophage infection, while RpfA and RpfB showed differential requirements, with MontyDev requiring both and Bora dependent on RpfB.
Conclusion: Our data suggest potential interactions between mycobacteriophage proteins and host cell wall transglycosylases during infection.

Keywords: resuscitating promoting factors, lytic mycobacteriophages, *Mycobacterium smegmatis*, peptidoglycan, lytic transglycosylases

Introduction

The emergence of drug-resistant tuberculosis (TB) threatens to undermine global TB control.[1,2] Drug resistant strains require protracted treatment with expensive drugs that are associated with poor treatment outcomes and adverse side-effects.[3] Hence, alternative therapeutics such as bacteriophages have been explored and gained much attention for the treatment of several recalcitrant antimicrobial resistant infections.[4–7] Bacteriophages are also inherently noninfectious to humans and, therefore, are attractive therapeutics for drug-resistant infections.[8,9]

Bacteriophages are classified as virulent or temperate. While temperate bacteriophages can enter a lysogenic lifestyle in which they integrate into the genome of the host and replicate via cell division, virulent bacteriophages exclusively induce lysis.[10] Although some bacteriophages have a broad host range, many display high specificity for recognition of distinct receptors on the host bacterial cell wall for infection.[11] For bacteriophages infecting mycobacterial species, the cell wall presents a significant barrier to entry due to its complex structure comprised of mycolic acids, arabinogalactan and peptidoglycan (PG) layers.[12] Mycobacteriophages require enzymes that break the cell wall to enable DNA entry, replication and subsequent lysis. Consequently, the genomes of most mycobacteriophages encode such enzymes, including Lysin A and Lysin B that hydrolyse the PG and degrades the ester bond anchoring mycolic acids to arabinogalactan respectively as well as Holins that regulate the timing of lysis.[13–16] While there is emerging evidence pointing to mechanisms of bacteriophage systems, the contribution of bacterial host factors in response to infection is sparse. Recently, a lytic bacteriophage which colonizes a bacterium *Schaalia odontolytica* that resides in the oral cavity, was shown to exploit the host-encoded lytic transglycosylase (LT), facilitating bacteriophage binding and infection. This LT showed a high level of structural homology to the resuscitation promoting factor, RpfB, of *Mycobacterium tuberculosis*.[17] In mycobacteria the lysozyme-like transglycosylase domain in RpfB is predicted to cleave the glycan backbone of

[1]School of Pathology, Faculty of Health Sciences, University of the Witwatersrand and the National Health Laboratory Service, Johannesburg, South Africa.
[2]Illinois Wesleyan University, Bloomington, IL, USA.
[†]These authors contributed equally to the work.

PG to allow for the insertion of new PG units during bacterial replication.[18] Mycobacteria encode a multiplicity of LTs, in some instances up to five (designated as RpfA-RpfE in *M. tuberculosis*) that have demonstrated roles in the hydrolysis of bacterial PG.[19–21] Herein, we aimed to assess whether changes in the PG due to a lack of Rpf activity influenced susceptibility to two newly identified mycobacteriophages.

Materials and Methods

Bacterial strains and culture conditions

All bacterial strains and plasmids used in this study are listed in Table 1. *Escherichia coli* DH5α was grown in LB broth or on LB agar. *Mycobacterium smegmatis* strains were grown in 7H9 (Difco) Middlebrook supplemented with 0.5% glycerol, 0.2% glucose, 0.085% NaCl and 0.05% Tween-80 or tyloxapol or on 7H10 (Difco) agar medium supplemented with 0.5% glycerol, 0.2% glucose and 0.085% NaCl. Hygromycin was added at 200 μg/mL for *E. coli* and 50 μg/mL for *M. smegmatis* as needed.

Drug susceptibility and permeability testing

M. smegmatis mc^{2}155 strain (wildtype, WT), the *rpf* deletion mutant (Δ*rpf*) and the various *rpf* complemented derivatives (Table 1) were grown to exponential phase. Cultures were adjusted to optical density $(OD)_{600\ nm} = 0.4$, serially diluted (10^{-1} to 10^{-5}), and appropriate dilutions plated on 7H10 agar to assess colony forming units (CFU/mL). In addition, 10 μL of each dilution was aliquoted onto 7H10 media supplemented with 0.004% sodium dodecyl sulfate (SDS) or 3 μg/mL vancomycin and un-supplemented plates served as controls. The plates were incubated at 37°C for 4 days before scoring for growth. The experiment was performed in triplicate.

Growth kinetics of the M. smegmatis *wild type,* rpf *deletion mutant and complemented strains*

Triplicate cultures of the WT, Δ*rpf* and the various *rpf* complemented derivatives (Table 1) were inoculated at an $OD_{600\,nm}$ of 0.05 in 7H9 media with tyloxapol using overnight precultures grown in the same media. Cultures were incubated with shaking at 37°C and $OD_{600\,nm}$ was first measured 16 h, then at 3- and 16-h intervals over a 48-h period. The $OD_{600\,nm}$ measurements for the three biological replicates were averaged and plotted against time.

Preparation of M. smegmatis *for bacteriophage infection*

A single colony of each *M. smegmatis* strain was grown overnight in 5 mL of 7H9 medium at 37°C with shaking at 100 rpm. Pre-cultures were diluted 1:100 into 50 mL 7H9 and grown to mid log phase ($OD_{600\,nm} = 0.8$) or late log phase ($OD_{600\,nm} = 2$). Cultures were harvested by centrifugation at 4 500 × *g*, washed twice with 30 mL of mycobacteriophage (MP) buffer (10 mM Tris pH 7.5, 10 mM $MgSO_4$, 1 mM $CaCl_2$, and 68.5 mM NaCl), and resuspended in the appropriate volume of MP buffer to an $OD_{600\,nm}$ of 2.

Purification and amplification of mycobacteriophages

To isolate mycobacteriophages, 2 mL of soil samples were resuspended in 10 mL of MP buffer, shaken (200 rpm) for 2 h

Table 1. Plasmids and Strains Used in This Study

	Description, markers, and/or genotype	*Source*
Plasmids		
pMV-RPFAB	L5 mycobacteriophage-based integrating shuttle phasmid based on pMV306 containing *rpfA* and *rpfB*; *hyg*, $attP_{L5}$-*int,* Hyg^R	19
pHINT-int-bla	pHINT-based suicide plasmid. *Eco*RI to *Nde*I excision of $attP_{L5}$ and *hyg bla*; int_{L5}, Ap^R	22
pMV-RPFABΔint	pMV-RPFAB derivative. Internal deletion with BsrGI and AvrII in the *int* gene. *rpfA; hyg,* Hyg^R	This work
pMV-RPFAΔint	pMV-RPFABΔint derivative. Internal HpaI to StuI excision of the *rpfB* gene. *rpfA*; *hyg*, Hyg^R	This work
pMV-RPFBΔint	pMV-RPFABΔint derivative. Internal StuI to MluI excision of the *rpfA* gene. *rpfB*; *hyg,* Hyg^R	This work
Strains		
E. coli DH5α	Strain used for routine cloning; *supE44 ΔlacU169 (ϕ80 lacZΔM15) hsdR17 recA1 endA1 gyrA96 thi-1 relA1*	Laboratory stock
mc^{2}155 (WT)	*ept-1* (efficient plasmid transformation) mutant of mc^{2}6	23
Δ*rpf*	*Mycobacterium smegmatis* quadruple *rpf* deletion mutant carrying internal -in-frame deletions in *rpfA*, *rpfB*, *rpfE1* and *rpfE2*	19
Δ*rpf*+RpfAB^{Mtb}	*Msm* Δ*rpf* carrying *rpfA* and *rpfB* in pTT-RPFABΔi and integrated at the $attP_{Tweety}$ site, Km^R	22
Δ*rpf*+RpfCDE^{Mtb}	*Msm* Δ*rpf* carrying *rpfC*, *rpfD* and *rpfE* in pH-RPFCDEΔi and integrated at the $attP_{L5}$ site, Hyg^R	22
Δ*rpf*+RpfABCDE^{Mtb}	*Msm* Δ*rpf* carrying *rpfA* and *rpfB* in pTT-RPFABΔi integrated at the $attP_{Tweety}$ site and *rpfC*, *rpfD* and *rpfE* in pH-RPFCDEΔi integrated at the $attP_{L5}$ site, Km^R, Hyg^R	22
Δ*rpf*+RpfA^{Mtb}	*Msm* Δ*rpf* carrying *rpfA* in pMV-RPFAΔint and integrated at the $attP_{L5}$ site, Hyg^R	This work
Δ*rpf*+RpfB^{Mtb}	*Msm* Δ*rpf* carrying *rpfB* in pMV-RPFBΔint and integrated at the $attP_{L5}$ site, Hyg^R	This work

Ap^R, ampicillin-resistant; Hyg^R, hygromycin-resistant; Km^R, kanamycin-resistant; Rpf, resuscitation-promoting factor; WT, wildtype.

at 37°C and the supernatant filtered using a Membrane filtration (MF)-Millipore® Membrane 0.22 μm filter. Ten 50 μL aliquots were mixed with 450 μL of the WT strain ($OD_{600\,nm}$ = 2) at room temperature for 30–60 min. Following addition of 4.5 mL of Mycobacteriophage top agar (MPTA), mixtures were overlaid on 7H10 plates and incubated at 37°C for 2–3 days. MPTA contains 7H9 (Difco) Middlebrook liquid medium, supplemented with 1.14% LB-agar, 0.2% glycerol, 0.2% glucose, 0.085% NaCl, and 0.1% $CaCl_2$. Single plaques were picked and resuspended in 1 mL of MP buffer. The suspension was filtered, serially diluted (10^{-1}–10^{-10}) and 450 μL of WT cells were added to 50 μL of each dilution of the mycobacteriophage (multiplicity of infection [MOI] 1:10, mycobacteriophage to bacteria) to ascertain the dilution yielding confluent ('lacey') plaques. High titer lysate was prepared by overlaying several 'lacey' plates with 3 mL of MP buffer each and incubating the plates for 4–6 h at room temperature with intermittent manual agitation. The pooled mycobacteriophage suspensions were collected, filter sterilized and the plaque-forming units (PFU)/mL assessed as described above. The mycobacteriophage lysates were stored at 4°C.

Mycobacteriophage Infection of *M. smegmatis* Wild Type, *Rpf* Deletion Mutant, and Complemented Strains

High titer lysates of both mycobacteriophages were serially diluted (10^0–10^{-10}) to confirm PFU/mL. Infections were performed at a MOI of 1:10 (mycobacteriophage:bacteria). Following 15–60 min of adsorption at room temperature, mixtures were combined with MPTA and overlaid on 7H10 plates. Plates were incubated at 37°C for 2–3 days and PFUs/mL were calculated and presented as a percentage relative to the WT strain.

Adsorption assays

A single colony of the WT, Δ*rpf*, and Δ*rpf*::*rpf*AB, was inoculated in 10 mL of 7H9 medium and incubated overnight at 37°C with shaking at 100 rpm. Pre-cultures were diluted 1:100 in 100 mL and grown overnight to mid log phase ($OD_{600\,nm}$ = 0.8) or late log phase ($OD_{600\,nm}$ = 2). Cells were harvested by centrifugation at 4 500 × *g*, washed twice with 40 mL of MP buffer and the pellets resuspended in the appropriate volume of MP to $OD_{600\,nm}$ of 2. For infection, 2.7 mL aliquot of each strain was mixed with 300 μL of high titer mycobacteriophage lysate ($\sim 10^9$ PFU/mL) at an MOI of 1:10 and incubated at 37°C with gentle shaking at 30 rpm. At time points 0-, 15-, 30-, 60-, 90-, and 120-min post infection, 300 μL of the mycobacteriophage cell suspension was collected, vortexed for 5 s where appropriate and centrifuged at 20,000 × *g* for 30 s. Supernatant containing unadsorbed bacteriophages, was carefully aspirated, diluted serially (10^0–10^{-10}), and 50 μL of each dilution was used to infect 450 μL WT cells (OD_{600} = 2). After 15 min of incubation at room temperature, MPTA overlays were poured on 7H10 plates. Plates were incubated at 37°C for 2–3 days and the percentage PFU/mL relative to WT was calculated with data representing the average of three biological repeats.

Negative staining transmission electron microscopy

Transmission electron microscopy was performed at the Electron Microscope Unit, University of Cape Town, South Africa. Briefly, carbon-coated copper grids (Agar Scientific, UK) were made hydrophilic using a EMS100 Glow Discharge Unit (Electron Microscopy Sciences, USA). Samples were applied to the grids and negatively stained with 2% uranyl acetate (SPI Supplies, USA). Imaging was performed on a FEI T20 transmission electron microscope (Thermo Fisher [formerly FEI], Eindhoven, Netherlands) at 200 kV and images were collected using a Gatan US 1000 CCD camera (Ametek Inc., USA).

Extraction, whole genome sequencing, and annotation of mycobacteriophage DNA

Details are provided in the Supplementary Data.

Construction of M. smegmatis *strains expressing single* M. tuberculosis rpfA *or* rpfB *homologues*

In a previous study, we generated the pMV-RPFAB integrating plasmid with *rpfA* and *rpfB* genes from *M. tuberculosis*.[19] This vector was further manipulated to generate pMV-RPFAΔint and pMV-RPFBΔint, as described in the Supplementary Data.

Data analysis

Graphs and figures were generated using Microsoft PowerPoint, Excel, GraphPad Prism (version 10.2.3) or Biorender.com software. GraphPad Prism (version 10.2.3) was used for all statistical analysis and data comparisons.

Results

Isolation, purification, and characterization of lytic mycobacteriophages

Two mycobacteriophages were isolated from damp soil collected in Johannesburg, South Africa: MontyDev from under a lavender bush (Benoni, GPS co-ordinates –26.1777°, 28.2838°) and Bora from a flowerbed (Braamfontein, GPS co-ordinates –26.1947°, 28.0323°). Both mycobacteriophages formed circular, turbid zones of clearance, on a lawn of WT *M. smegmatis* cells, with MontyDev ~1–2 mm (Fig. 1A) and Bora in ~1 mm in size (Fig. 1B). Transmission electron microscopy revealed that both mycobacteriophages are *siphoviral* with long, non-contractile tails (Fig. 1C and D). MontyDev has a ~71 nm diameter icosahedral capsid and a ~284 nm long tail, whereas Bora has a prolate capsid, measuring ~163 nm long and ~40 nm wide, with a ~247 nm long tail.

Genomic analysis of mycobacteriophages MontyDev and Bora

Whole genome sequencing confirmed that both mycobacteriophages are *siphoviral* with MontyDev in cluster R and Bora in cluster O. No integrase genes were detected in both the genomes, suggesting they are virulent mycobacteriophages. Neither mycobacteriophage genome contain tRNA or tmRNA reading frames. Predicted gene functions include structural, packaging, DNA replication, lytic, packaging and assembly, and hypothetical proteins (Supplementary Table S1). MontyDev has 71,250 bp, a G + C content of 56.0%, 101 predicted open reading frames, of which 70 (69.3%) are hypothetical proteins. All

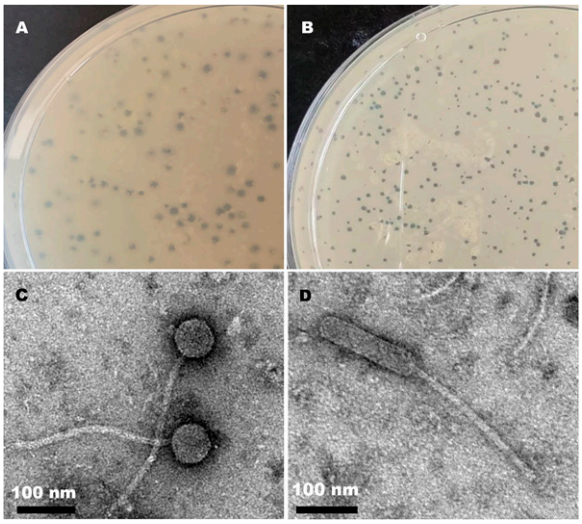

FIG. 1. Characterization of mycobacteriophage plaque morphology and virion morphotype. **(A)** Plaques produced by phage MontyDev on a lawn of WT. **(B)** Plaques produced by phage Bora on a lawn of WT. **(C)** Mycobacteriophage MontyDev virions contain a ~71 nm wide icosahedral head and a non-contractile tail with a length of ~284 nm. **(D)** Mycobacteriophage Bora virions contain a ~163 nm long and ~40 nm wide prolate head, and a non-contractile tail with a length of ~247 nm. WT, wildtype.

open reading frames except one (MONTYDEV_42) are transcribed from the forward, positive strand (Fig. 2A, Supplementary Table S1). The genome of Bora has 71,494 bp, a G + C content of 65.3%, and 124 predicted open reading frames, of which 82 (66.1%) are hypothetical proteins. Of these 124 genes, 54 are transcribed from the forward and 70 from the reverse strand (Fig. 2B, Supplementary Table S1). Both MontyDev and Bora contain the endolysins Lysin A and Lysin B, while the Holin protein is present only in Bora (Fig. 2A and B, Supplementary Table S1). Sequencing and annotation information for both mycobacteriophages is available at the Sequence Read Archive (BioProject numbers PRJNA1108268 and PRJNA1108264, respectively), the Actinobacteriophage Database (https://phagesdb.org) under https://phagesdb.org/phages/MontyDev/ and https://phagesdb.org/phages/Bora/, and Genbank (Accessions numbers PP763599 and PP763600, respectively).

Susceptibility of M. smegmatis *strains with and without* rpfs *to MontyDev and Bora*

We previously generated *M. smegmatis* strains in which a mutant (Δ*rpf)* devoid of all its chromosomal *rpf* genes (*rpfA*, *rpfB*, *rpfE* and *rpfE2*) was complemented with combinations of the five *M. tuberculosis rpf* genes with their cognate promoters.[22] In our prior work, we generated a set of plasmids containing different combinations of the *rpf* genes from *M. tuberculosis*. The homology between *M. tuberculosis* and *M. smegmatis rpfA* and *rpfB* alleles at the protein level is high (see Supplementary Fig. S1). The *rpfA* gene from the two organisms share a 44.7% identity (entire length of 515 amino acids [aa]) with a 90.7% similarity in transglycosylase domain PF06737 (68/75 aa), whilst the *rpfB* alleles share a 74.4% identity (entire length 375 aa), with 90.7% similarity in transglycosylase domain PF06737 (68/75 aa). AlphaFold predictions for RpfA generate space filling models which all contain the conserved PF06737 domain (blue, high confidence in ribbon model; green block, low expected error) (Supplementary Fig. S2). RpfA and RpfB show highly conserved predictions for the entire length of the protein, while RpfC, RpfD, and RpfE contain the conserved PF06737 domain flanked by regions of lower confidence (Supplementary Fig. S2).

We first infected the various strains with MontyDev at a MOI of 1:10 to assess the role of *rpf* genes for mycobacteriophage infection. The Δ*rpf* mutant and the Δ*rpf* complemented with RpfCDE^{Mtb} (Δ*rpf*::RpfCDE^{Mtb}) yielded lower PFUs/mL compared to WT (Fig. 3A). However, combinatorial addition of *rpfAB*^{Mtb} to Δ*rpf* (Δ*rpf*::RpfAB^{Mtb}) showed a significant recovery in PFUs/mL, albeit still less than WT. The addition of *rpfAB*^{Mtb} to Δ*rpf*::RpfCDE^{Mtb} to generate a strain containing all the *M. tuberculosis rpf*s (Δ*rpf*::RpfABCDE^{Mtb}) resulted in similar plaques levels as Δ*rpf*::RpfAB^{Mtb} suggesting that RpfA and RpfB together contribute to mycobacteriophage infection (Fig. 3A).

To evaluate the individual role of RpfA and RpfB in bacteriophage infection, each gene from *M. tuberculosis* was cloned into integrative plasmids and electroporated into Δ*rpf* to generate strains Δ*rpf*::RpfA^{Mtb} and Δ*rpf*::RpfB^{Mtb}, respectively (Table 1). Quantitative polymerase chain reaction (PCR) confirmed the expression of the introduced genes in Δ*rpf* (Supplementary Fig. S3). Only expression of *rpfA* and *rpfB* was assessed in WT since *M. tuberculosis* does not have the equivalent of the *M. smegmatis rpfE* and *rpfE2* homologues. In *M. smegmatis*, expression of the *rpfA*^{Msm} transcript was ~10-fold higher than the *rpfB*^{Msm} transcript (Supplementary Fig. S3). Complemented Δ*rpf* strains expressed all *M. tuberculosis rpf* genes, albeit at varying degrees. We expected some differences in *rpf* gene expression in the recombinant *M. smegmatis* strains, as native *M. tuberculosis* promoters were used. Indeed, the *rpfC*^{Mtb} transcript was most abundant, while expression of the remaining *M. tuberculosis* genes was more comparable in each of the complemented strains, and to the *M. smegmatis rpfA* and *rpfB* genes (Supplementary Fig. S3). Despite these variations, our prior work using these heterologous complemented strains restored biofilm forming defects in *M. smegmatis rpf* deficient mutants.[19] Based on these data we tested the effect of *rpf* gene deletion on drug susceptibility and permeability. The Δ*rpf* mutant showed a 2–3 log reduction in growth in the presence of 3 μg/mL vancomycin and 0.004% SDS which was rescued by *rpfA* and *rpfB* individually and in combination to WT levels (Supplementary Fig. S4). Comparison of growth kinetics showed no significant viability defect between the Δ*rpf* and the three complemented strains Δ*rpf*::RpfAB^{Mtb}, Δ*rpf*::RpfA^{Mtb} and Δ*rpf*::RpfB^{Mtb}. The WT strain displayed a small but significant difference in growth rate between 10 and 30 h; however, this difference was subsequently abrogated. The WT strain showed reduced growth in stationary phase; however, this was minor and likely due to clumping that routinely occurs in mycobacterial cultures at this stage of growth (Supplementary Fig. S5).

Both Δ*rpf*::RpfA^{Mtb} and Δ*rpf*:RpfB^{Mtb}, when infected with cluster R mycobacteriophage MontyDev, showed increased plaque formation, compared to Δ*rpf* (~25% vs. ~10%).

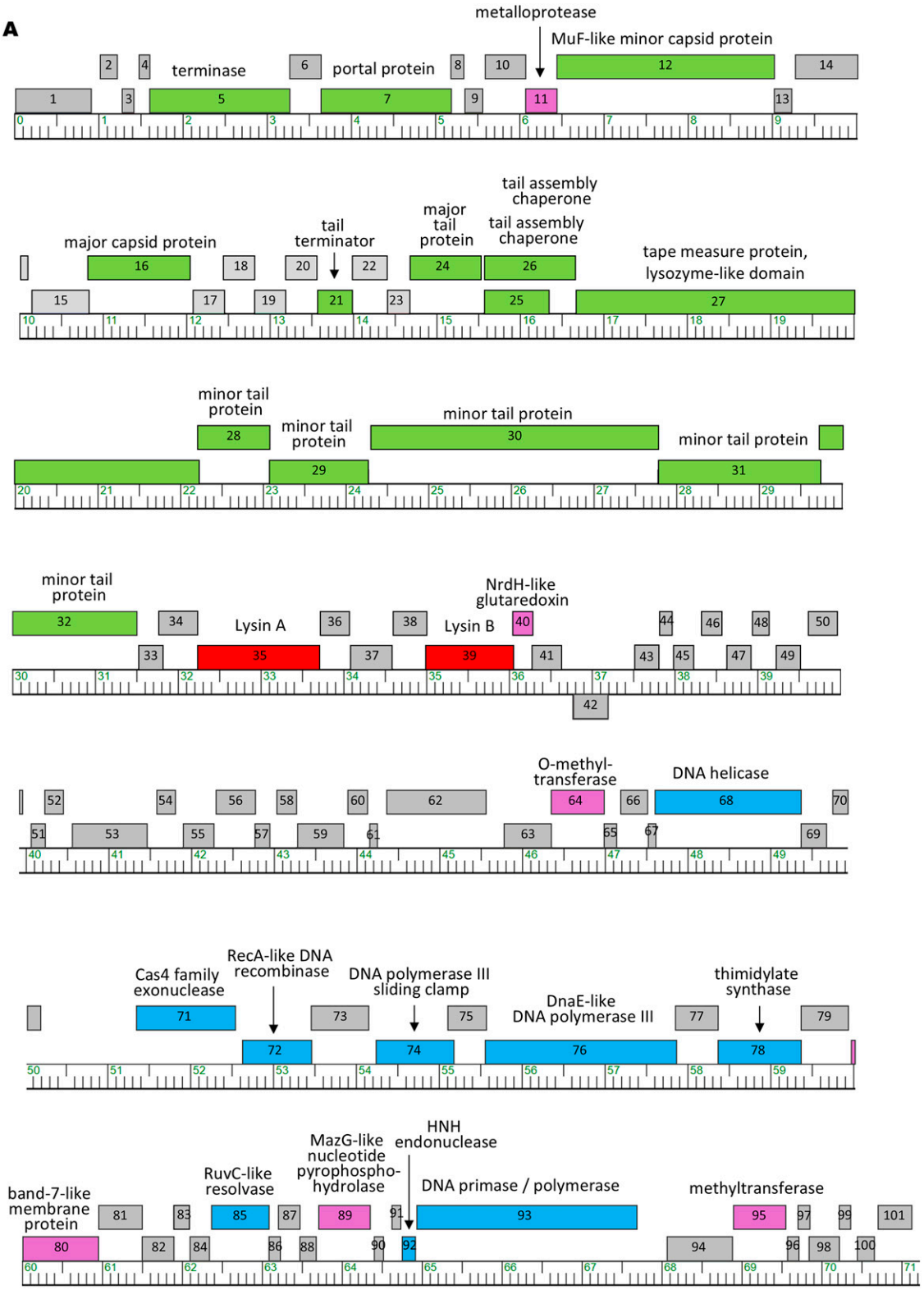

FIG. 2. Graphic representation of the genomes of mycobacteriophages MontyDev and Bora. The images were produced based on output from the Phamerator website (https://phamerator.org/phages). Nomenclature follows the guidelines as stipulated at the SEA-PHAGES Program (https://phagesdb.org/media/workflow/protocols/pdfs/Function_Assignments_best.pdf). **(A)** The genome of MontyDev (Cluster R) comprises 71,250 bp and 101 predicted genes. **(B)** The genome of Bora (Cluster O) comprises 71,494 bp and 124 predicted genes. Peptidoglycan lytic genes in these genomes are Lysin A (MONTYDEV_35 and BORA_64) Holin (BORA_66), tape measure protein (MONYTDEV_27) and minor tail protein, D-ala-D-ala carboxypeptidase (BORA_57). Lysin B (MONTYDEV_39 and BORA_65) breaks the ester bond between arabinogalactan and the mycolic acid layer. Blocks represent predicted open reading frames. Those above the ruler are transcribed in the forward orientation, below the ruler in reverse orientation. Colors: green, structural function; blue, nucleic acid metabolic function; red, lytic function; purple, other function; gray, hypothetical protein/unknown function.

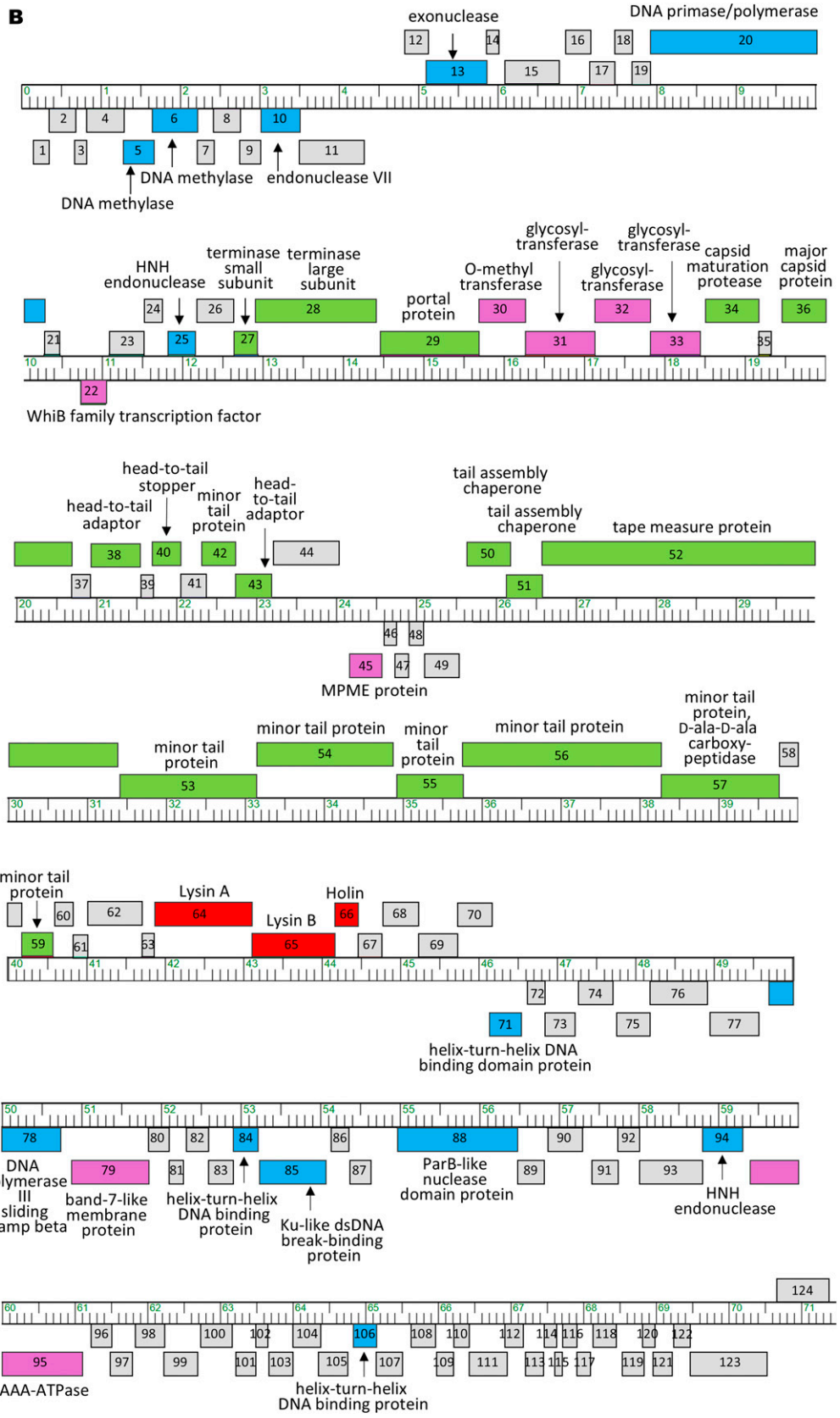

FIG. 2. (*Continued*).

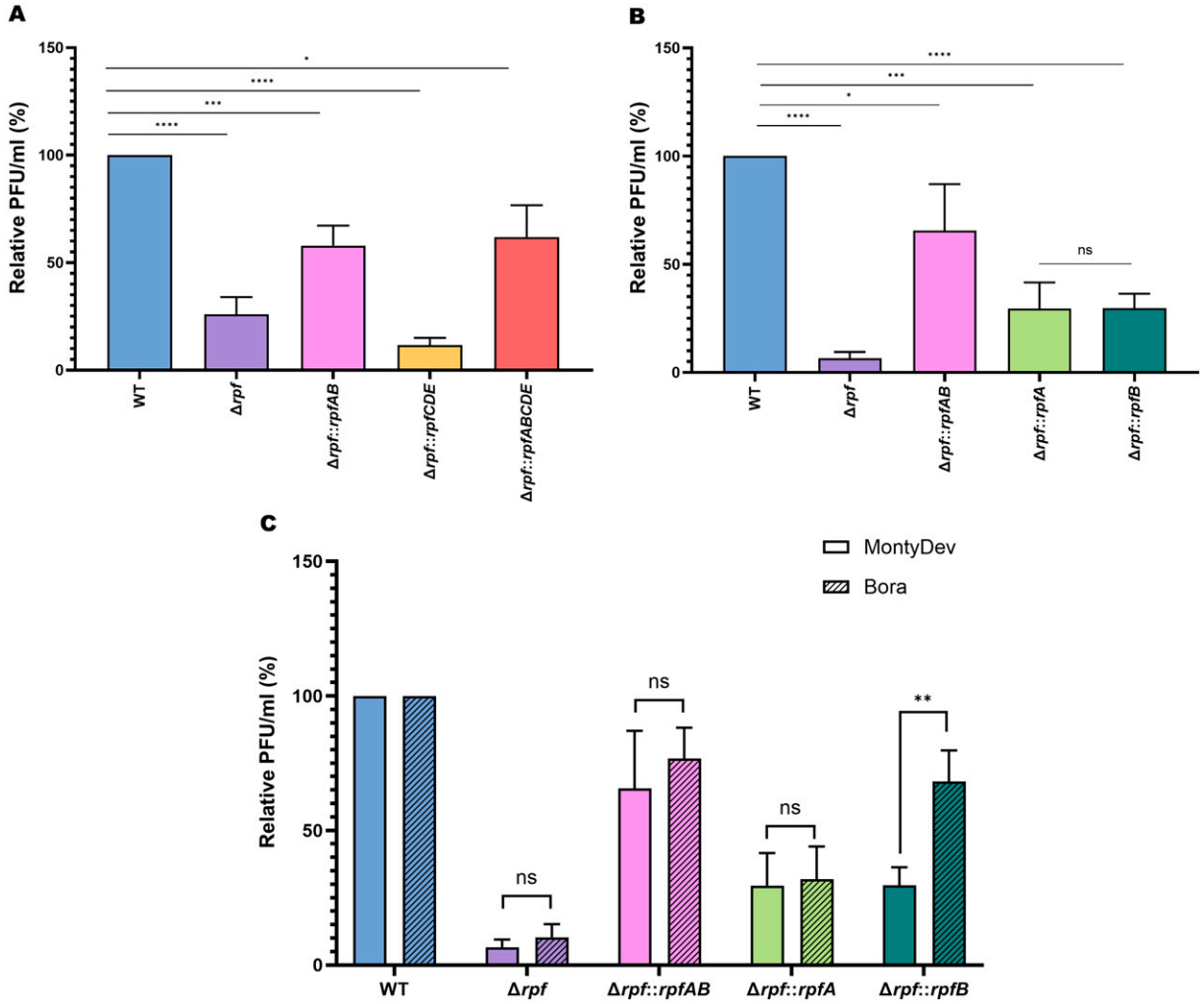

FIG. 3. Infection of *Mycobacterium smegmatis* strains with lytic phages MontyDev and Bora. The mycobacteriophages were incubated with the respective bacterial cells at a MOI of 1:10 (1 mycobacteriophage:10 bacteria) and allowed to adsorb for at least 15 min. PFU were assessed by mixing the bacteriophage and cell suspension with top agar and overlaid on 7H10 plates. **(A)** Bar graph depicting normalized PFU in the WT, Δ*rpf* mutant, and the Δ*rpf* mutant complemented with combinations of *rpf*A–E infected with MontyDev. **(B)** Bar graph depicting normalized PFU in the WT, Δ*rpf* mutant, and the Δ*rpf* mutant complemented with combinations of *rpf*A and *rpfB* infected with MontyDev. **(C)** Comparison of the plaque forming units for WT, Δ*rpf* mutant, and the Δ*rpf* mutant complemented with combinations of *rpfA* and *rpfB* infected with MontyDev (open bars) and Bora (hatched bars). Error bars indicate standard error of the mean of three experiments. $*p < 0.05$, $**p < 0.01$, $***p < 0.005$, $****p \leq 0.0001$ and ns = not significant. Graphs were generated using GraphPad Prism software, version 10. MOI, multiplicity of infection; PFU, plaque forming units; Rpf, resuscitation-promoting factor.

However, Δ*rpf*::RpfAB^{Mtb} showed more than double the plaque-forming ability compared with the single gene complements, indicating synergy between RpfA and RpfB (Fig. 3B). To assess if this synergy was broadly applicable in mycobacteriophages, we tested the susceptibility of the cluster O mycobacteriophage, Bora (Fig. 3C). Infection of Δ*rpf*::RpfAB^{Mtb} again yielded similar increased plaque-forming ability as observed with MontyDev, i.e., partial complementation of Δ*rpf* (∼75%). However, the plaque-forming ability of Bora in Δ*rpf*::RpfB^{Mtb} was comparable to that of Δ*rpf*::RpfAB^{Mtb} (∼65% vs ∼75%), while the Δ*rpf*::RpfA^{Mtb} resulted in lower but similar levels of PFU/mL for both MontyDev and Bora (∼25%) (Fig. 3C).

To determine if the reduction in PFU/mL observed for the Δ*rpf* mutant was due to an adsorption defect, we adapted an assay that monitors adsorption of phage over a period of 120 min,[24] in mid and late log phase ($OD_{600\,nm}$ = 0.8 and $OD_{600\,nm}$ = 2.0, respectively), shown in Figure 4A. While MontyDev showed no adsorption differences between strains grown to late log phase, Bora exhibited some variation in adsorption under the same conditions. However, none of these differences reached statistical significance (Fig. 4B and C). To account for possible difference in cell wall structure for late log phase cells, we also tested adsorption at a lower optical density ($OD_{600\,nm}$ = 0.8, corresponding to mid log phase) and included a vortexing step to remove unbound bacteriophage. Under these conditions MontyDev showed a marginal reduction in adsorption with the Δ*rpf* mutant after 60 min compared with WT, an effect that was reversed with genetic complementation however, these differences were not statistically significant (Fig. 4D). Bora displaced comparable levels of adsorption with the wild type (Fig. 4E).

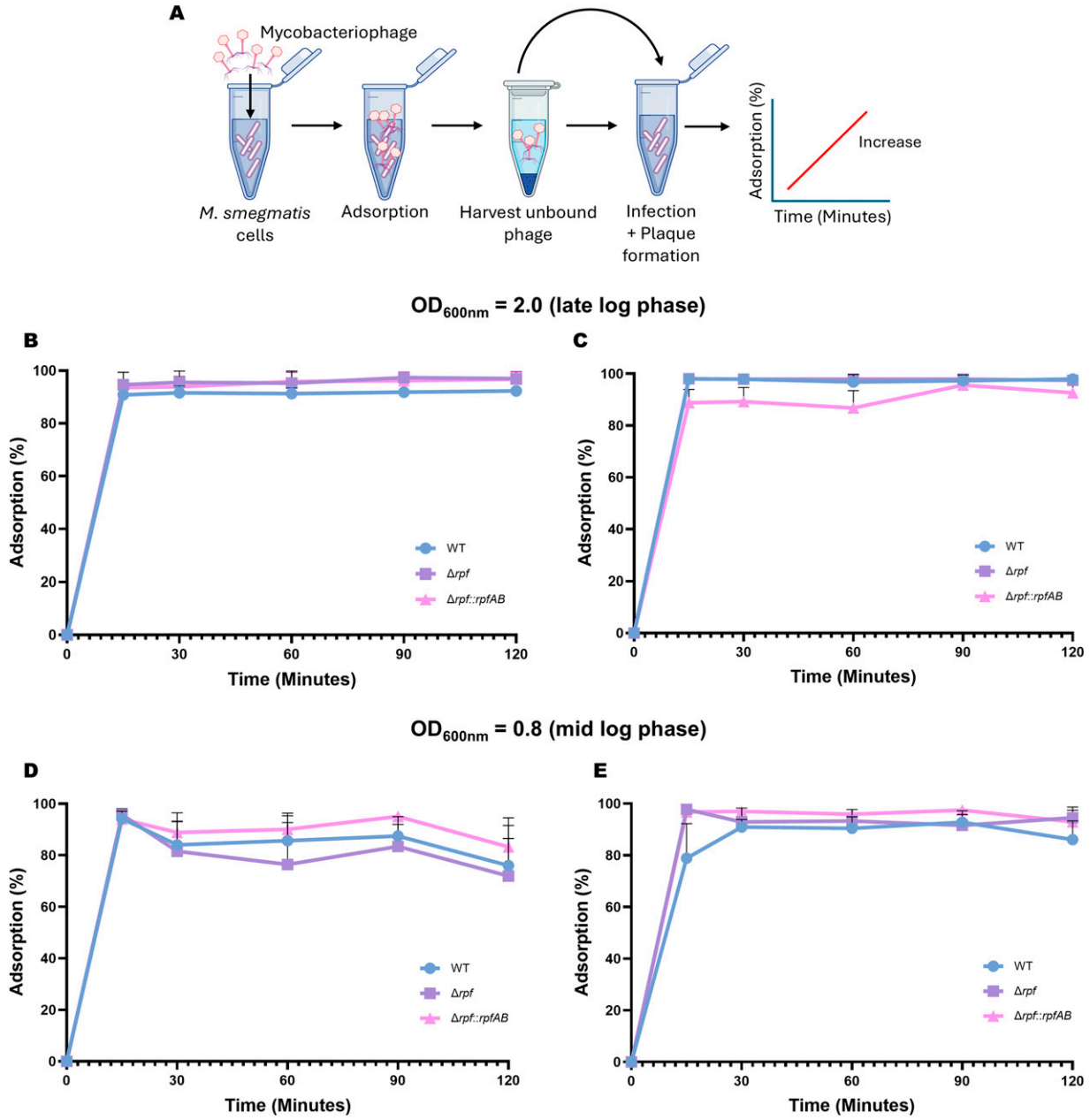

FIG. 4. Comparison of adsorption of mycobacteriophages to *Mycobacterium smegmatis* cells in mid and late log growth phase. **(A)** Schematic representation of the mycobacteriophage adsorption assay. Bacteriophages were incubated with bacterial cells at a MOI of 1:10 (1 mycobacteriophage:10 bacteria) and allowed to adsorb over a 120-min period. At various time points, samples were removed and the unbound bacteriophages in the supernatant were harvested and reinfected into the WT strain to quantify residual, unabsorbed bacteriophages. PFU were assessed by mixing the suspension with top agar and overlaid on 7H10 plates. Adsorption assessment of MontyDev **(B)** and Bora **(C)** in the WT, Δ*rpf* mutant, and the Δ*rpf* mutant complemented with *rpfAB* grown to late-log phase ($OD_{600\ nm}$ = 2.0) over a 120-min incubation period. Adsorption assessment of MontyDev **(D)** and Bora **(E)** with the WT, Δ*rpf* mutant, and the Δ*rpf* mutant complemented with *rpfAB* grown to mid-log phase ($OD_{600\ nm}$ = 0.8) over a 120-min incubation period. In these experiments a 5 second vortex step was included at each sampling point prior to centrifugation of the samples to remove loosely bound mycobacteriophages. The experiments were conducted in triplicate and the data are presented as percent (%) mycobacteriophage adsorbed over time. Error bars indicate standard error of the mean of three experiments. Graphs were generated using GraphPad Prism software, version 10.

Discussion

Mycobacteriophages infecting *M. tuberculosis* and nontuberculous mycobacteria are gaining interest as novel adjunctive treatments for drug resistant infections.[25–27] Understanding mycobacteriophages and their interactions with specific host factors is key for potential clinical applications.[11] Despite bacteriophage genomes being relatively small (~15 to ~500 kbp), many bacteriophage genes are annotated as hypothetical proteins, based on bioinformatic and computational tools to other bacteriophages. Assigning specific biological function to these proteins could advance

our understanding of phage–host interactions and resistance mechanisms.

Mycobacteria have multiple *rpf* genes, with four representatives in *M. smegmatis* (*rpfA*, *rpfB*, *rpfE*, and r*pfE2*) and five in *M. tuberculosis* (*rpfA-E*).[28] We exploited a *M. smegmatis* mutant strains lacking all *rpf* genes and various complemented derivatives thereof expressing various combinations of *M. tuberculosis rpf* genes, to investigate how host encoded *rpf* genes affect susceptibility to MontyDev and Bora. Infection of Δ*rpf* with these mycobacteriophages resulted in a significant reduction in PFU/mL compared with WT, indicating decreased vulnerability to infection in the absence of *rpf* genes. Strains complemented with *rpfA* and *rpfB* together (but not *rpfC*, *rpfD* and *rpfE*), showed partial restoration of susceptibility to MontyDev (cluster R). To further delineate the role of *rpfA* and *rpfB*, complemented derivatives containing either *rpfA* or r*pfB* separately also showed increased susceptibility to MontyDev compared to Δ*rpf*, but not to the level observed with combined complementation with *rpfA* and *rpfB*. For Bora (cluster O), a complemented derivative containing *rpfB* alone, increased plaque formation compared to the strain containing *rpfA* only, though not to the level of WT. Our data suggest that MontyDev requires both *rpfA* and r*pfB*, while Bora is more dependent on *rpfB* for optimal mycobacteriophage infection. Our previous work demonstrated that deletion of all four Rpf homologues in *M. smegmatis* reduced muropeptides production and altered PG crosslinking, effects which were reversed by simultaneous complementation with $rpfA^{Mtb}$ and $rpfB^{Mtb}$.[19] In this context, the growth defect of the *rpf* deficient mutant strain in the presence of vancomycin and SDS was fully rescued with *rpfA* and *rpfB,* individually and in combination to WT levels. Despite these changes, the *rpf* deletion mutant maintained viability, exhibiting growth kinetics comparable with both WT and complemented strains.

The reduction in PFU observed with the Δ*rpfAB* double mutant could be owed to receptor masking, preventing mycobacteriophage adhesion due to structural changes in the PG or disruption of protein interactions between mycobacteriophages and host. To test this, we performed adsorption assays but observed no differences in bacteriophage binding between strains for either mycobacteriophage during mid and late log growth phases of the cells.

A bioinformatic analysis of Lysin A proteins from 224 sequenced mycobacteriophages revealed that these enzymes are widespread, diverse and extensively modular, featuring functional domains such as *N*-terminal peptidases, amidases, muramidases or transglycosylases, and *C*-terminal putative cell wall binding domains.[29,30] Lysin B proteins, cleave the ester bonds between arabinogalactan and mycolic acids in the mycobacterial cell wall, but are not present in all mycobacteriophages.[29,30] Many mycobacteriophage genomes also encode Holin proteins that span the cell membrane and allow Lysins to pass into the extracellular milieu.[30] Coordinated timing achieved by disruption of the proton motive force across the cell membrane releases the Lysins to start hydrolysis of the PG layer and disrupt the mycobacterial outer membrane simultaneously, leading to cell death and bacteriophage release.[31,32]

In light of the broad repertoire of enzymes involved in bacteriophage DNA entry and lysis, we examined how mycobacteriophages MontyDev and Bora infect *M. smegmatis* mutants lacking LT activity. Both mycobacteriophages are *siphoviral* but differ in their arsenal of genes encoding PG lytic activity. MontyDev has PG-degrading activity in Lysin A (MONTYDEV_35), in two distinct domain, i.e., a *N*-terminal L-alanyl-D-glutamate peptidase domain (M15_C family) and a *C*-terminal lysozyme-like domain (GH_19 superfamily). The PG degradation of Bora potentially involves two proteins: Lysin A (BORA_64), with a predicted *N*-acetylmuramoyl-L-alanine amidase domain (Ami_2 family), and a minor tail protein with a D-ala-D-ala carboxypeptidase domain (S11 family, BORA_57). The genomes of both mycobacteriophages encode a Lysin B, but only Bora contains the Holin gene, operonic with Lysin A and Lysin B, which is typical for cluster O bacteriophages.[14] Generally, Lysin B is positioned either immediately downstream of Lysin A, or it is separated by a maximum of four genes, often encoding putative Holin proteins in some bacteriophages.[33,34] Although MontyDev displayed this genetic arrangement, the three hypothetical proteins separating Lysin A and Lysin B do not contain any predicted genetic domains typical of Holins or other lysis proteins, suggesting that it accesses the periplasmic space by yet an unidentified mechanism(s).

PG-hydrolysing motifs corresponding to peptidase and transglycosylase activities located within TMPs of bacteriophages has also been shown to be a common strategy employed by bacteriophages infecting Gram-positive bacterial hosts.[35,36] Our analysis revealed that the TMP of MontyDev contains a lysozyme-like domain however, the role of this protein in this mycobacteriophage is unclear. Lysin B from related bacteriophages have shown broad activity against various mycobacterial species[37–40] and, when combined with anti-TB drugs, can target drug-resistant *M. tuberculosis* in macrophages without harming host cells.[41] Conversely, the bacteriophage LC001 exploited a host LT, similar to the mycobacterial RpfB protein to enhance receptor binding and infection in the bacterium *Schaalia odontolytica*.[17] *M. tuberculosis* PG remodeling enzymes have also been shown to interact transiently with other proteins such as RpfB and the D,L-endopeptidase, Rpf interacting protein A (RipA) to remodel PG.[21] Similarly, mycobacteriophage proteins may exploit host Rpf proteins to facilitate cell lysis.

Conclusion

In summary, our data suggest that mycobacteriophages from different clusters have differential requirements for Rpf proteins in mycobacteria, while our research suggests that Rpf activity is required for mycobacteriophage infection, the exact molecular mechanism(s) by which mycobacteriophage enzymes interact with host encoded Rpf proteins to cleave PG remains to be fully elucidated.

Acknowledgment

The authors thank Deborah Jacobs-Sera, Daniel A. Russell, and Graham F. Hatfull (Department of Biological Sciences, University of Pittsburgh, Pittsburgh, PA, USA) for their technical support related to the raw sequence analysis and genome annotations. The authors thank Mohamed Jaffer (Electron Microscope Unit at the University of Cape Town, Cape Town, South Africa) for assistance with microscopy and

Inqaba Biotec, a commercial next generation sequencing service provider, for assistance with whole-genome sequencing. The authors also thank Danishka Moodley, Dhanishta Patel, Serene Keenan, Yuveshni Chetty and Astika Sewcharran for their technical support.

Authors' Contributions

Conceptualization: B.D.K., B.G.G., C.S.E., and E.E.M. Data curation; C.M., K.G., and N.S. Formal analysis: C.M., C.S.E., E.E.M., and B.G.G. Funding acquisition: B.D.K. Investigation: C.M., K.G., N.S., and B.G.G. Methodology and validation: B.G.G., C.S.E., C.M., E.E.M., K.G., and N.S. Project administration: B.G.G., C.S.E., and E.E.M. Resources: B.D.K. Software: Not Applicable. Supervision: B.G.G., B.D.K., C.S.E., and E.E.M. Visualization: Not Applicable; Writing—original draft: B.G.G. Writing—review and editing: B.G.G., B.D.K., C.S.E., C.M., E.E.M., K.G., and N.S.

Author Disclosure Statement

No competing financial interests exist.

Funding Information

This study was supported with funds from the South African Department of Science and Innovation and the National Research Foundation (DCOE015).

Supplementary Material

Supplementary Data
Supplementary Figure S1
Supplementary Figure S2
Supplementary Figure S3
Supplementary Figure S4
Supplementary Figure S5
Supplementary Table S1

References

1. Dookie N, Rambaran S, Padayatchi N, et al. Evolution of drug resistance in *Mycobacterium tuberculosis*: A review on the molecular determinants of resistance and implications for personalized care. J Antimicrob Chemother 2018; 73(5):1138–1151.
2. Liebenberg D, Gordhan BG, Kana BD. Drug resistant tuberculosis: Implications for transmission, diagnosis, and disease management. Front Cell Infect Microbiol 2022;12:943545.
3. Lange C, Aarnoutse RE, Alffenaar JWC, et al. Management of patients with multidrug-resistant tuberculosis. Int J Tuberc Lung Dis 2019;23(6):645–662.
4. Chang RYK, Nang SC, Chan HK, et al. Novel antimicrobial agents for combating antibiotic-resistant bacteria. Adv Drug Deliv Rev 2022;187:114378.
5. Liu C, Hong Q, Chang RYK, et al. Phage-Antibiotic therapy as a promising strategy to combat multidrug-resistant infections and to enhance antimicrobial efficiency. Antibiotics (Basel) 2022;11(5):570.
6. Luong T, Salabarria AC, Roach DR. Phage therapy in the resistance era: Where do we stand and where are we going? Clin Ther 2020;42(9):1659–1680.
7. O'Flaherty S, Ross RP, Coffey A. Bacteriophage and their lysins for elimination of infectious bacteria. FEMS Microbiol Rev 2009;33(4):801–819.
8. Abedon ST. Bacteriophage clinical use as antibacterial "Drugs": Utility and precedent. Microbiol Spectr 2017;5(4):1–26.
9. Abedon ST. Use of phage therapy to treat long-standing, persistent, or chronic bacterial infections. Adv Drug Deliv Rev 2019;145:18–39.
10. Kimchi O, Meir Y, Wingreen NS. Lytic and temperate phage naturally coexist in a dynamic population model. Isme J 2024;18(1).
11. Clokie MR, Millard AD, Letarov AV, et al. Phages in nature. Bacteriophage 2011;1(1):31–45.
12. Shaku M, Ealand C, Matlhabe O, et al. Peptidoglycan biosynthesis and remodeling revisited. Adv Appl Microbiol 2020;112:67–103.
13. Abeysekera GS, Love MJ, Manners SH, et al. Bacteriophage-encoded lethal membrane disruptors: Advances in understanding and potential applications. Front Microbiol 2022;13:1044143.
14. Catalao MJ, Gil F, Moniz-Pereira J, et al. Diversity in bacterial lysis systems: Bacteriophages show the way. FEMS Microbiol Rev 2013;37(4):554–571.
15. Ealand C, Machowski EE, Jacobs O, et al. Complete genome sequence of lopsy, a B1 cluster mycobacteriophage. Microbiol Resour Announc 2023;12(7):e0033323.
16. Machowski EE, Ealand CS, Jacobs O, et al. Complete genome sequence of Azrael100, a V cluster mycobacteriophage. Microbiol Resour Announc 2023;12(10):e0068423.
17. Cen L, Chang Y, Bedree JK, et al. Exploitation of a bacterium-encoded lytic transglycosylase by a human oral lytic phage to facilitate infection. J Virol 2022;96(17):e0106322.
18. Vollmer W, Bertsche U. Murein (peptidoglycan) structure, architecture and biosynthesis in *Escherichia coli*. Biochim Biophys Acta 2008;1778(9):1714–1734.
19. Ealand C, Rimal B, Chang J, et al. Resuscitation-Promoting factors are required for *Mycobacterium smegmatis* biofilm formation. Appl Environ Microbiol 2018;84(17):e00687–e00618.
20. Hett EC, Chao MC, Rubin EJ. Interaction and modulation of two antagonistic cell wall enzymes of mycobacteria. PLoS Pathog 2010;6(7):e1001020.
21. Hett EC, Chao MC, Steyn AJ, et al. A partner for the resuscitation-promoting factors of *Mycobacterium tuberculosis*. Mol Microbiol 2007;66(3):658–668.
22. Gordhan BG, Peters JS, McIvor A, et al. Detection of differentially culturable tubercle bacteria in sputum using mycobacterial culture filtrates. Sci Rep 2021;11(1):6493.
23. Snapper SB, Melton RE, Mustafa S, et al. Isolation and characterization of efficient plasmid transformation mutants of *Mycobacterium smegmatis*. Mol Microbiol 1990;4(11):1911–1919.
24. Wetzel KS, Illouz M, Abad L, et al. Therapeutically useful mycobacteriophages BPs and Muddy require trehalose polyphleates. Nat Microbiol 2023;8(9):1717–1731.
25. Dedrick RM, Guerrero-Bustamante CA, Garlena RA, et al. Engineered bacteriophages for treatment of a patient with a disseminated drug-resistant Mycobacterium abscessus. Nat Med 2019;25(5):730–733.
26. Dedrick RM, Smith BE, Cristinziano M, et al. Phage therapy of mycobacterium infections: Compassionate use of phages in 20 patients with drug-resistant mycobacterial disease. Clin Infect Dis 2023;76(1):103–112.

27. Hatfull GF. Mycobacteriophages: Windows into tuberculosis. PLoS Pathog 2014;10(3):e1003953.
28. Machowski EE, Senzani S, Ealand C, et al. Comparative genomics for mycobacterial peptidoglycan remodelling enzymes reveals extensive genetic multiplicity. BMC Microbiol 2014;14:75.
29. Broendum SS, Buckle AM, McGowan S. Catalytic diversity and cell wall binding repeats in the phage-encoded endolysins. Mol Microbiol 2018;110(6):879–896.
30. Payne KM, Hatfull GF. Mycobacteriophage endolysins: Diverse and modular enzymes with multiple catalytic activities. PLoS One 2012;7(3):e34052.
31. Grabowski Ł, Łepek K, Stasiłojć M, et al. Bacteriophage-encoded enzymes destroying bacterial cell membranes and walls, and their potential use as antimicrobial agents. Microbiol Res 2021;248:126746.
32. Pollenz RS, Bland J, Pope WH. Bioinformatic characterization of endolysins and holin-like membrane proteins in the lysis cassette of phages that infect Gordonia rubripertincta. PLoS One 2022;17(11):e0276603.
33. Hatfull GF. The secret lives of mycobacteriophages. Adv Virus Res 2012;82:179–288.
34. Pimentel M. Genetics of phage lysis. Microbiol Spectr 2014;2(1):MGM2–M2013.
35. Pedulla ML, Ford ME, Houtz JM, et al. Origins of highly mosaic mycobacteriophage genomes. Cell 2003;113(2):171–182.
36. Piuri M, Hatfull GF. A peptidoglycan hydrolase motif within the mycobacteriophage TM4 tape measure protein promotes efficient infection of stationary phase cells. Mol Microbiol 2006;62(6):1569–1585.
37. Loeffler JM, Nelson D, Fischetti VA. Rapid killing of *Streptococcus pneumoniae* with a bacteriophage cell wall hydrolase. Science 2001;294(5549):2170–2172.
38. Schuch R, Nelson D, Fischetti VA. A bacteriolytic agent that detects and kills *Bacillus anthracis*. Nature 2002; 418(6900):884–889.
39. Yoong P, Schuch R, Nelson D, et al. Identification of a broadly active phage lytic enzyme with lethal activity against antibiotic-resistant *Enterococcus faecalis* and *Enterococcus faecium*. J Bacteriol 2004;186(14):4808–4812.
40. Zimmer M, Vukov N, Scherer S, et al. The murein hydrolase of the bacteriophage phi3626 dual lysis system is active against all tested *Clostridium perfringens* strains. Appl Environ Microbiol 2002;68(11):5311–5317.
41. Singh AK, Gangakhedkar R, Thakur HS, et al. Mycobacteriophage D29 Lysin B exhibits promising anti-mycobacterial activity against drug-resistant *Mycobacterium tuberculosis*. Microbiol Spectr 2023;11(6):e0459722.

Address correspondence to:
Bhavna Gowan Gordhan, PhD
National Health Laboratory Service
Cnr DeKorte and Hospital Streets
Braamfontein
Johannesburg 2000
South Africa

Email: Bhavnaben.gordhan@wits.ac.za

Bavesh Davandra Kana, PhD
National Health Laboratory Service
Cnr DeKorte and Hospital Streets
Braamfontein
Johannesburg 2000
South Africa

Email: Bavesh.kana@wits.ac.za